The effects of UV radiation in the marine environment

Edited by

STEPHEN DE MORA
IAEA Marine Environment Laboratory, Monaco

SERGE DEMERS
ISMER, Rimouski, Québec

and

MARIA VERNET
University of California at San Diego

Contents

○ ○

1

○ ○

Enhanced UV radiation – a new problem for the marine environment

Robert F. Whitehead, Stephen J. de Mora* and Serge Demers

1.1 Introduction

UV irradiance at the earth's surface is intimately related to stratospheric ozone. This gas tends to be concentrated in the lower stratosphere (hence the notion of an ozone layer) and is primarily responsible for the absorption of solar UV radiation (UVR). UVR has been recognised for many years (e.g. Worrest, Dyke & Thomson, 1978; Worrest *et al.*, 1981; Calkins, 1982) as a potential stress for organisms in a variety of environments and as a factor in biogeochemical cycling (Zepp, Callaghan & Erickson, 1995). The trend in recent years of an intensifying, but periodic, anthropogenic-induced decline in stratospheric ozone concentrations with concurrent enhanced UV-B radiation is quite alarming. Altered solar radiation regimes can potentially upset established balances in marine ecosystems and thus presents a new problem. Most attention has been given to the 'ozone hole' over Antarctica that has been recorded annually since the 1980s. However, recent observations have confirmed measurable ozone losses over other regions, including the development of an Arctic ozone hole. The major factor responsible for the destruction of the ozone layer is anthropogenic emissions of chlorofluorocarbons (CFCs). These gases, having no natural sources, are non-toxic and inert in the troposphere, but are photolysed in the stratosphere, thereby releasing reactive chlorine atoms that catalytically destroy ozone. Other anthropogenic contributions to ozone depletion may include global changes in land use and the increased emission of nitrogen dioxide as a result of fertiliser applications (Bouwman, 1998). Paradoxically, the anthropogenic emissions of greenhouse gases that tend to cause a temperature increase at the earth's surface also produce a decrease in stratospheric temperatures. This decrease in stratospheric temperatures leads to enhanced formation of polar stratospheric clouds and may serve to increase ozone

loss in polar regions (Salawitch, 1998; Shindell, Rind & Lonergan, 1998).

The understanding of the atmospheric chemistry involved in ozone depletion has greatly expanded since the link to CFCs was first proposed in 1974 (Molina & Rowland, 1974). A worldwide network of ozone observation stations has documented continuing ozone reductions over many areas of the globe. The effects have been especially pronounced in the Antarctic region, where an ozone hole, characterised by the depletion of 60% or more of the ozone, opens up each spring over an area that is now slightly larger than the size of Canada (Smith *et al.*, 1992). In the Arctic and into the North Temperate Zone, the ozone layer diminished by 15% to 20% during the 1991–2 winter[1]. The increases in atmospheric carbon dioxide anticipated over the next 50 years should lead to stratospheric cooling, thereby accelerating the destruction of stratospheric ozone and perhaps leading to an Arctic ozone hole as severe as that over Antarctica (Austin, Butchart & Shine, 1992). The latest Environmental Canada (Wardle *et al.*, 1997) report indicates ozone loss over the Arctic of up to 45% during the spring of 1997 in response to atmospheric conditions that may be indicative of changes due to stratospheric cooling (Mühler *et al.*, 1997; Wardle *et al.*, 1997). The magnitude of ozone destruction is predicted to increase over the next century despite international efforts to reduce the usage and emission of CFCs in accordance with the Montreal Protocol (Shindell *et al.*, 1998).

Regardless of the cause, the decrease in stratospheric ozone concentrations provokes an increase of UV-B radiation in the wavelength range 280 to 320 nm (Crutzen, 1992; Smith *et al.*, 1992; Kerr & McElroy, 1993). For example, an annual increase in UV-B of up to 35% has been observed in Canada for the winter–spring period during 1989–93 (Kerr & McElroy, 1993). The UV-B wave band represents less that 0.8 % of the total energy reaching the surface of the earth but is responsible for almost half of the photochemical effects in the aquatic and marine environments. Although not widely recognised due to a lack of field measurements, biologically effective levels of solar UVR penetrate water columns to significant depths: at least 30 m for UV-B (280–320 nm) and 60 m for UV-A (320–400 nm) (Smith & Baker, 1979; Holm-Hansen, Lubin & Helbing, 1993). Even in highly productive lakes and coastal regions, UVR can penetrate to at least 20 m (Kirk, 1994b; Scully & Lean, 1994) and this penetration increases as stratospheric ozone declines (Smith *et al.*, 1992).

---

[1] A number of articles on Arctic ozone and atmospheric chemistry can be found in *Science* (1993) **261**.

The environmental impact of this rise in solar UV-B has recently become a source of much concern and speculation in public as well as scientific literature.

Solar UV-B radiation is known to have a wide range of harmful effects, generally manifested as reduced productivity, on freshwater and marine organisms, including bacterioplankton and phytoplankton (Vincent & Roy, 1993; Cullen & Neale, 1994; Booth *et al.*, 1997). Analogous studies on zooplankton and on the early life history stages of fishes indicate that exposure to relatively low levels of UV-B also deleteriously affects these groups (Holm-Hansen *et al.*, 1993). All plant, animal and microbial groups appear to be susceptible to UV-B, but to a highly variable extent that depends on the individual species and its environment (Vincent & Roy, 1993). In addition, UV-B may have significant effects on community structure that are not apparent through studies based on individual species or trophic levels (e.g. Bothwell, Sherbot & Pollock, 1994; Vernet *et al.*, 1994).

This chapter provides an introduction to some fundamental aspects of the behaviour of solar radiation in the atmosphere and water column. The fate of photons is also considered in respect of basic photochemistry and photobiology. The introduction is intended to form a basis for the understanding of the relationships amongst anthropogenic-related changes in the atmosphere, changes in solar radiation and the new problems they present to marine ecosystems. Subsequent chapters elucidate effects on specific biological structures and organisms, trophic-level interactions, photochemical reactions and biogeochemical cycling.

1.2   The solar spectrum and the nature of light

The effect of solar radiation on chemical and biological processes in the marine environment depends on both intensity and spectral distribution. There is significant natural variability in the factors that attenuate solar radiation and UV-B in both the atmosphere and the ocean. At the edge of the earth's atmosphere, the solar energy reaching a surface perpendicular to the radial direction from the sun is approximately 1394 W m^{-2} and has a spectrum characterised as UV (UV-C 200–280 nm, UV-B 280–320 nm, UV-A 320–400 nm), photosynthetically available radiation (PAR 400–700 nm) and infrared (IR > 700 nm) (Figure 1.1). The energy characteristic of each wavelength is determined by the relationship:

$$E = hc/\lambda \qquad\qquad (1.1)$$

where E is the energy in joules, h is the Planck constant, c is the speed of light, and λ is the wavelength in metres. When dealing with biological and chemical systems, the most commonly used unit is the mole photon (also called an Einstein) which contains N photons (where N is Avogadro's number $= 6.023 \times 10^{23}$). The radiant energy of 1 mole photon is defined by:

$$E_{\text{(mole photon)}} = Nhc/\lambda = 1.19629 \times 10^8 \text{ J}/\lambda \qquad (1.2)$$

Thus, the energy of a mole photon varies inversely with wavelength (Figure 1.2). For example, the energy of 1 mole photon of 300 nm light is 398 kJ. In contrast, the energy of 1 mole photon of 700 nm light is only 171 kJ. The large increase in energy with decreasing wavelength has important chemical and biological implications when one is considering systems under changing solar spectral distributions.

1.3   Attenuation of solar energy

1.3.1   Attenuation in the atmosphere

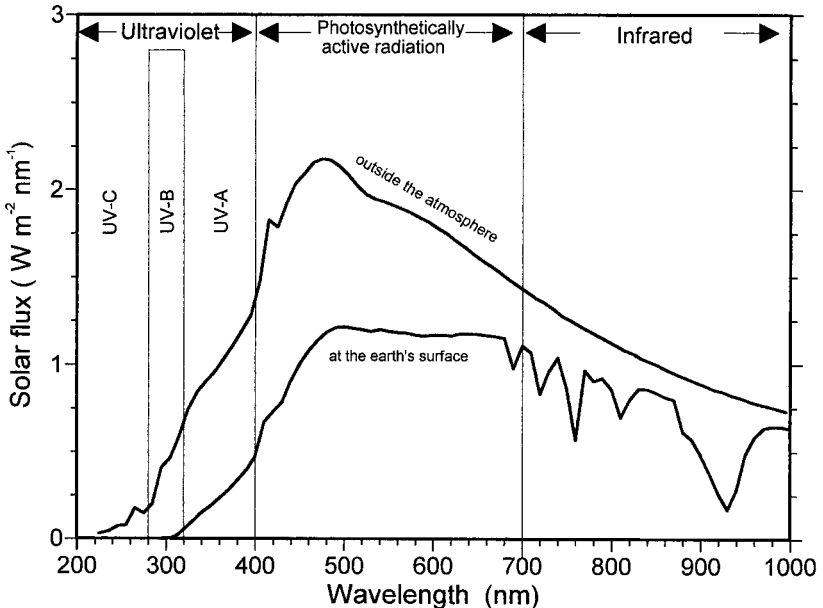In general terms, the relative solar spectral distribution outside the

Figure 1.1.   General characteristics of solar radiation outside the atmosphere and at the earth's surface.

atmosphere comprises 51% in the IR region, 41% in the visible (PAR) region and 8% in the UV region (Figure 1.3). Passing through the atmosphere, the radiation is subject to scattering and absorption which reduces its intensity by ∼35% before it reaches the earth's surface. As a result, the spectral distribution at the earth's surface differs from that experienced at the edge of the atmosphere and is a combination of direct and diffuse radiation. The amount of scattering and absorption is a function of the atmospheric composition (gases and particles) and the pathlength of the photons through the atmosphere. Thus, given a uniform atmospheric composition the spectral distribution and intensity would still vary as a function of solar zenith angle (i.e. time of day, season and latitude). A typical solar spectral distribution for a low latitude (30° N) site on a sunny day with the sun at zenith is composed of about 43% IR, 52% PAR and 5% UV radiation. For the same location with a zenith angle of 60° or 79°, the distribution changes to about 45% IR, 52% PAR and 3% UV radiation or 53% IR, 46% PAR and 1% UV, respectively (Figure 1.3). The reason for the larger relative reduction at the UV end of the spectrum
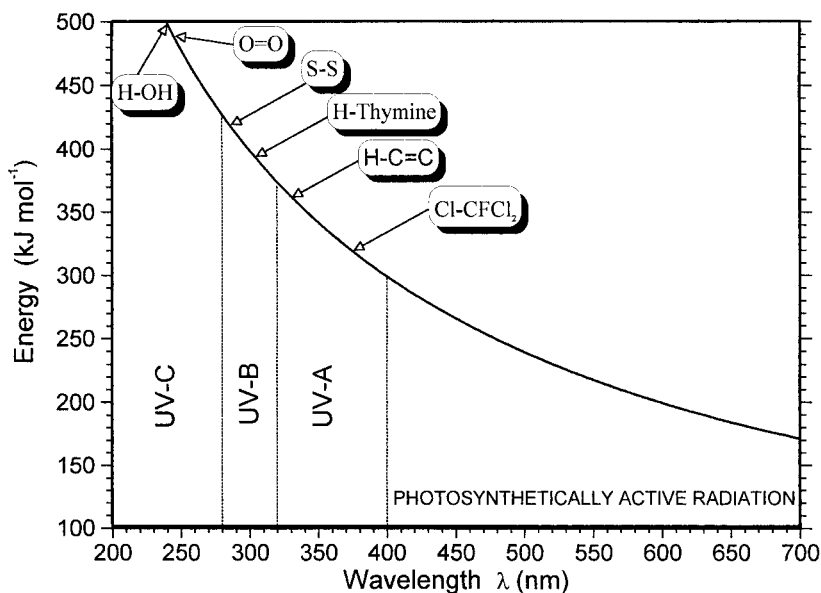

Figure 1.2. The inverse relationship between energy per mole and wavelength of solar radiation. Bond dissociation energies of some important biomolecular bonds are indicated by the location of the arrows on the curve.

with increasing atmospheric pathlength is two-fold:

1. *Enhancement of scattering*: Scattering in the atmosphere is inversely proportional to the fourth power of the wavelength and is therefore more effective in the UV region. Scattering may redirect a photon's path away from the earth such that it is lost back to space or may enhance the probability of absorption due to longer pathlengths.
2. *Enhancement of absorption*: UV radiation < 320 nm is strongly absorbed by ozone and to some extent by oxygen (Figure 1.4). Longer pathlengths effectively increase the total ozone encountered by a photon and thereby enhances the probability of absorption.

1.3.1.1 Absorbance of UV and the ozone cycle
The strong reduction in UVR (< 320 nm) reaching ground level (Figure 1.1) is due primarily to absorption by ozone and oxygen. Although ozone is a trace gas in the atmosphere (maximum concentration ~ 8 parts per
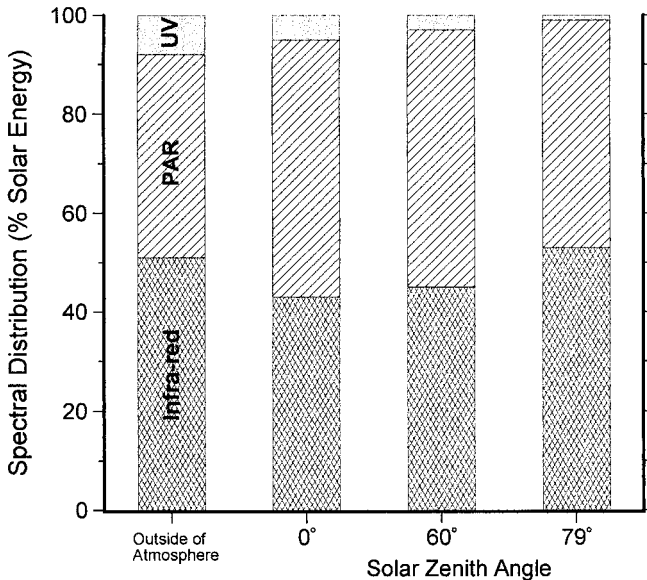
Figure 1.3. Spectral distributions of wavelength regions as a percentage of total solar radiation. Bars represent solar radiation outside the atmosphere and at the earth's surface (30° N) for three solar zenith angles. Atmospheric attenuation causes the largest relative reduction at the UV end of the spectrum.

million by volume (ppmv) at $\sim 35\,km$ altitude), the attenuation of UV by ozone is orders of magnitude higher than that of oxygen. The absorption of UV with enough energy to break the O=O bond ($\Delta H = 494\,kJ\,mol^{-1}$ requires $\lambda < 240\,nm$) is the first step in the production of ozone (O_3):

$$O_2 + hv(\lambda < 240\,nm) \rightarrow O + O \qquad [1.1]$$

where v is the wave frequency.
The O atoms released may then react with O_2 to form O_3:

$$2(O + O_2 + M \rightarrow O_3 + M) \qquad [1.2]$$

where M is a collision chaperone that absorbs excess energy but is itself unreactive. Net ozone production is $3\,O_2 \rightarrow 2\,O_3$. Ozone can be destroyed by direct photolysis:

Figure 1.4. Spectral characteristics of the absorbance cross-sections of oxygen (O_2) and ozone (O_3) at 298 K. Whereas wavelengths in the UV-C and UV-B regions are strongly absorbed by O_3, UV-A and PAR are little affected. (Data from Inn & Tanaka, 1953; Molina & Molina, 1986.)

$$O_3 + h\nu(\lambda < 410\,\text{nm}) \rightarrow O + O_2 \qquad [1.3]$$

or by recombination with O:

$$O_3 + O \rightarrow 2\,O_2 \qquad [1.4]$$

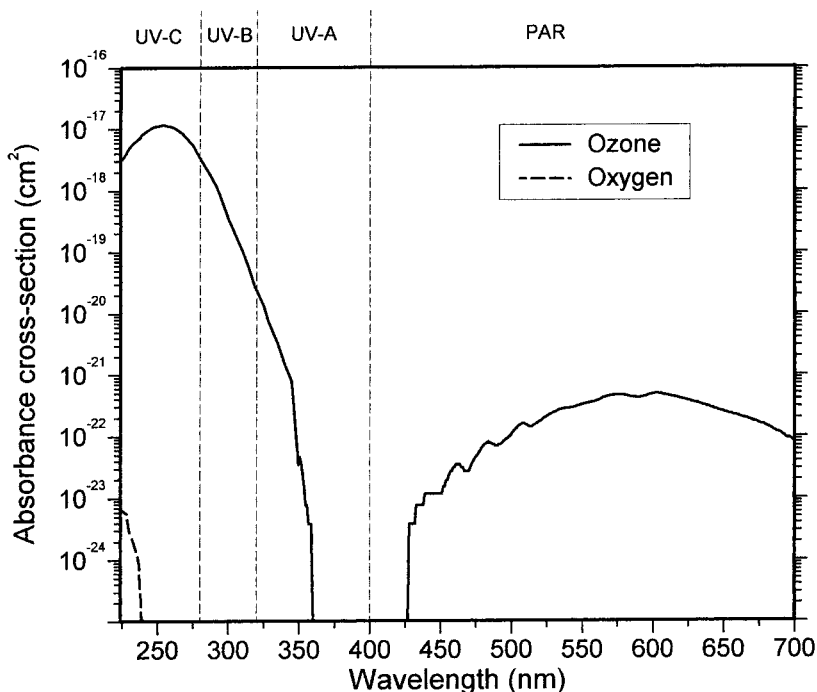Net ozone destruction is thus $2\,O_3 \rightarrow 3\,O_2$.

However, at all times the concentration of oxygen far exceeds that of ozone and the recombination reaction is slower than production. If pure oxygen reactions were the only mechanism for ozone production and destruction, the ozone layer would be approximately twice as thick as is currently observed. Thus, other destruction reactions are necessary to explain natural ozone levels.

The rate of recombination is greatly enhanced by catalytic cycles of the general form involving a free radical, X:

$$O_3 + X \rightarrow XO + O_2 \qquad [1.5]$$
$$O + XO \rightarrow O_2 + X \qquad [1.6]$$

or

$$O_3 + XO \rightarrow 2\,O_2 + X \qquad [1.7]$$

where X may be NO, HO, Cl, I or Br. The X species are regenerated in this sequence and may be involved in as many as 100 000 ozone-destroying cycles before being sequestered into less active reservoir species by slower reactions such as:

$$HO + NO_2 \rightarrow HNO_3 \qquad [1.8]$$
$$XO + NO_2 \rightarrow XONO_2 \qquad [1.9]$$
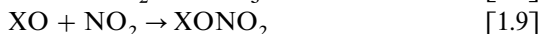
Stratospheric ozone levels are therefore maintained by a dynamic balance between photochemical production and destruction. Intuitively, one might expect to find the highest stratospheric ozone levels at low latitudes and high altitudes where solar irradiance is strongest. However, ozone levels are highest in the middle stratosphere over high latitudes and not the upper stratosphere above the equator. In fact, ozone levels above the equator are relatively constant at about 260 DU[2] whereas ozone levels above high latitudes in the northern hemisphere may reach 450 DU. The pattern is a result of the redistribution of high altitude ozone-rich air from the tropics to lower altitudes in the polar regions (Figure 1.5).

---

[2] 100 Dobson units, DU, are equivalent to an ozone layer 1 mm thick at $0\,^\circ\text{C}$ and 1 atm pressure.

The natural O_3 cycle can be perturbed by interactions with anthropogenic compounds, most notably CFCs (WMO, 1995). CFCs were first produced in the 1930s and were heralded as non-toxic, non-flammable compounds with a wide variety of uses as refrigerants, propellants for aerosol cans, cleaning compounds for electronic parts and blowing agents for foam manufacturing. Over the 50 years since the introduction of CFCs, their concentrations in the atmosphere, in general, have shown a steady increase, with a corresponding decrease in stratospheric ozone (Figure 1.6). Mario Molina and F. Sherwood Rowland first proposed their role in the destruction of atmospheric ozone in 1974. They shared the 1995 Nobel Prize for Chemistry with Paul Crutzen for their work in this field. The ozone hole over Antarctica was first reported in 1985 and led to work that has firmly established the link between CFCs and ozone depletion.

CFCs are quite stable and inert in the troposphere. They have long residence times in the atmosphere and are mixed into the stratosphere, attaining notable concentrations. Once in the stratosphere, CFCs are exposed to UV radiation of sufficient energy to break the carbon–chlorine bonds. The released chlorine can then attack O_3 in the following reaction sequence:

$$Cl + O_3 \rightarrow ClO + O_2 \qquad [1.10]$$
$$ClO + ClO \rightarrow Cl_2O_2 \qquad [1.11]$$
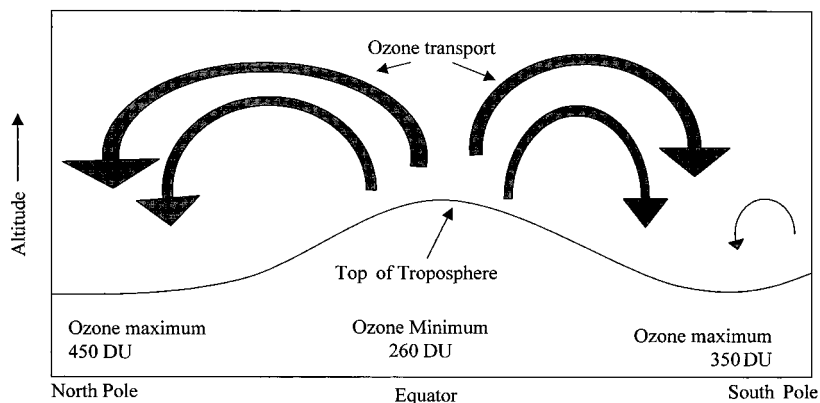$$Cl_2O_2 + hv \rightarrow Cl + ClOO \qquad [1.12]$$

Figure 1.5. Generalised atmospheric redistribution of O_3 without the influence of O_3 depletion. Highest O_3 production occurs over the equator and tropics, but atmospheric circulation transports the O_3 produced there towards the poles, giving rise to an O_3 maximum at higher latitudes. (Adapted from Stolarski, 1988.)

$$ClOO + O \rightarrow ClO + O_2 \qquad [1.13]$$
$$2 \times (Cl + O_3 \rightarrow ClO + O_2) \qquad [1.14]$$
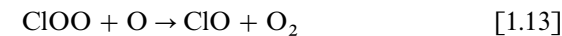
giving a net destruction of $2\,O_3 \rightarrow 3\,O_2$.

   These gas phase reactions can occur anywhere in the stratosphere, however, the rates are not sufficiently fast to explain the large ozone hole that has been observed in the spring over Antarctica since the early 1980s. In the gas phase reactions, reactive chlorine species (Cl, ClO) can be removed from the ozone destruction cycle and transformed into non-reactive reservoir chlorine compounds (HOCl, $ClONO_2$) by reactions [1.8] and [1.9]. A rapid conversion of reservoir chlorine into reactive chlorine is necessary to explain the ozone hole over Antarctica. The mechanism for this rapid conversion is heterogeneous (gas–solid) reactions catalysed on the surface of polar stratospheric clouds (PSCs). PSCs are composed largely of condensed nitric acid, which also reduce atmospheric NO_2 concentrations. Low NO_2 concentrations extend the life of reactive chlorine species by reducing the importance of reaction [1.9] in the gas
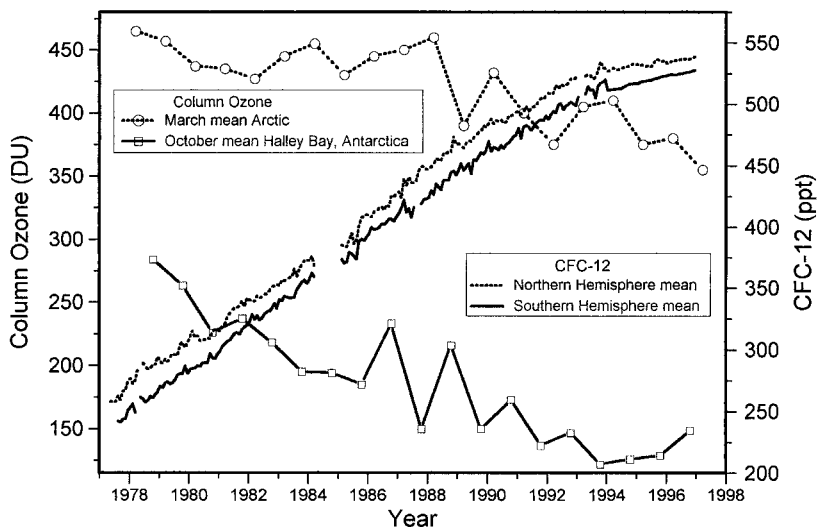
Figure 1.6. Comparison of the decrease in springtime stratospheric ozone over the Arctic and the Antarctic with the build-up of chlorofluorocarbon (CFC)12 in the northern and southern hemispheres. Natural atmospheric chlorine concentrations are relatively constant ($\cong 0.6$ p.p.b.v.) whereas anthropogenic sources have steadily increased since the introduction of CFCs. ppt, parts per trillion. (CFC data from Elkins, NOAA; Antarctic ozone from British Antarctic Survey; Arctic ozone from Environment Canada.)

phase. Surface-catalysed gas–solid reactions on PSCs causing the ozone hole are:

$$ClONO_{2(g)} + HCl_{(s)} \rightarrow Cl_{2(g)} + HNO_{3(s)} \qquad [1.15]$$
$$ClONO_{2(g)} + H_2O_{(s)} \rightarrow HOCl_{(g)} + HNO_{3(s)} \qquad [1.16]$$
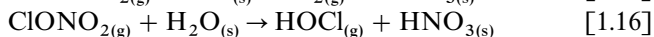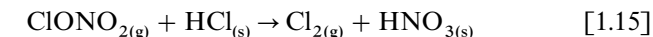
where subscript g denotes gas and s denotes solid.

The strong polar vortex that surrounds Antarctica during the winter reduces atmospheric exchange with lower latitudes and allows the build-up of stratospheric Cl_2 and HOCl. With the increase of solar radiation in the spring, the build-up of Cl_2 and HOCl released from the gas–solid reactions is photolysed and reactive Cl atoms are released to drive the catalytic ozone destruction. The process continues until the PSCs dissipate later in the spring due to stratospheric warming. Spring also brings a weakening of the polar vortex, which allows air with higher ozone concentration to invade from lower latitudes together with the advection of air with low ozone air away from Antarctica. An ozone hole of similar magnitude is not common over the Arctic because of a weaker polar vortex and higher average stratospheric temperatures that reduce PSCs formation in the early spring when there is sufficient sunlight for catalytic ozone destruction to occur. However, climatic changes in response to global warming may induce cooler stratospheric temperatures producing more PSCs (Pawson & Naujokat, 1997) and a stronger polar vortex over the Arctic (Chubachi, 1997). These conditions were observed in the winter/spring of 1995–6 and 1996–7 (Fioletov et al., 1997; Mühler et al., 1997), but it is too soon to determine whether this is a developing pattern or a transient event.

Outside Antarctica, ozone reductions are less dramatic but are still significant (Stolarski et al., 1992). The mechanism for ozone reduction at low and mid-latitudes is more equivocal than that for Antarctica (Pyle, 1997). Mass exchange of low ozone air across the polar vortex boundary could affect the global ozone budget. Heterogeneous gas–solid reactions might also occur outside the polar vortex. A ubiquitous layer of sulfate aerosols, partly of volcanic origin, may provide the necessary surfaces for the gas–solid reactions to occur (Hoffman & Solomon, 1989; Solomon et al., 1996). Atmospheric measurements indicate that the increase sulfate aerosols after the 1991 eruption of Mt Pinatubo did correlate with higher levels of reactive chlorine species and lower levels of nitrogen oxides (McCormick, Thomason & Trepte, 1995). Both observations suggest that sulfate aerosols may be sites of heterogeneous reactions. However, the

relative roles of chemical impacts of the sulfate layer and mass transport across the vortex boundary are still unresolved (Shepherd, 1997).

1.3.1.2   Effects on UV intensity and UV/PAR ratios

The absorbance cross-section of ozone increases by two orders of magnitude between 320 nm and the peak value at ~ 250 nm (Figure 1.4). A reduction in the ozone encountered by incoming solar radiation, either through ozone loss or reduced solar zenith angles, would first of all result in increased UV-B radiation (Madronich, 1991; Kerr & McElroy, 1993) (Figure 1.7a,b). In principle, UV-C would also increase, but absorption in this region is so efficient that a tremendous reduction in ozone is required in order for significant amounts to reach the earth's surface. As can be seen in Figure 1.4, UV-A is not affected by ozone absorption and PAR absorption is negligible compared to UV-B. The reduction of atmospheric O_3 causes two significant changes to ground-level UV-B, namely a shift in the spectrum towards shorter, more energetic wavelengths and an increase in intensity of the whole UV-B band (Figure 1.7a,b). Although the increase in integrated UV fluence due to ozone depletion in Antarctica (Figure 1.7b) is less than a factor of 5, the change in the ratio of low ozone irradiance to high ozone irradiance increases exponentially with decreasing UV-B wavelengths (Figure 1.7a). The shift in spectrum and the lack of significant effects in the UV-A and PAR regions also produces a change in the ratios of UV-B to UV-A and PAR. The change in the ratio of UV-B to PAR has been shown to be well correlated with ozone levels (Smith *et al.*, 1992). These changes in ratios are important to biological processes, as damage is usually associated with the shorter more energetic wavelengths whereas repair and photosynthesis require longer wavelengths (Cullen, Neale & Lesser, 1992).

1.3.1.3   Effects of clouds and particles

Atmospheric clarity and cloud cover can have a significant effect on UV radiation at ground level (Booth *et al.*, 1997). Atmospheric radiation modelling has shown that stratus clouds can reduce erythema-weighted UV radiation by up to 75% compared to clear sky conditions (350 DU O_3 and a solar zenith angle of 55°) (Tsay & Stamnes, 1992). This model also showed that cirrus clouds, stratospheric and tropospheric particles attenuated UV-B by 12%, 6%, and 5%, respectively. When ozone levels were reduced to 260 DU, stratus clouds still reduced UV-B levels to 56% less than in clear sky, 350 DU O_3 conditions. Under partly cloudy conditions, however, cumulus clouds have been shown to enhance total sky UV-B irradiance by up to 30% over short periods (Mimms &

(a)

Mawson Solar UVR Spectra

(b)

Mawson 1991
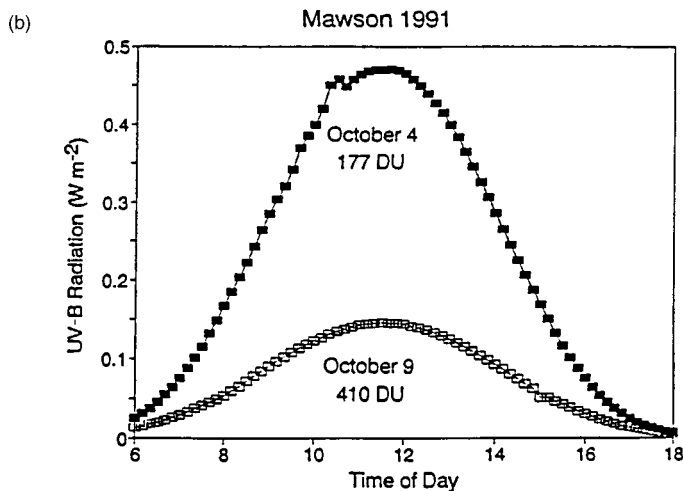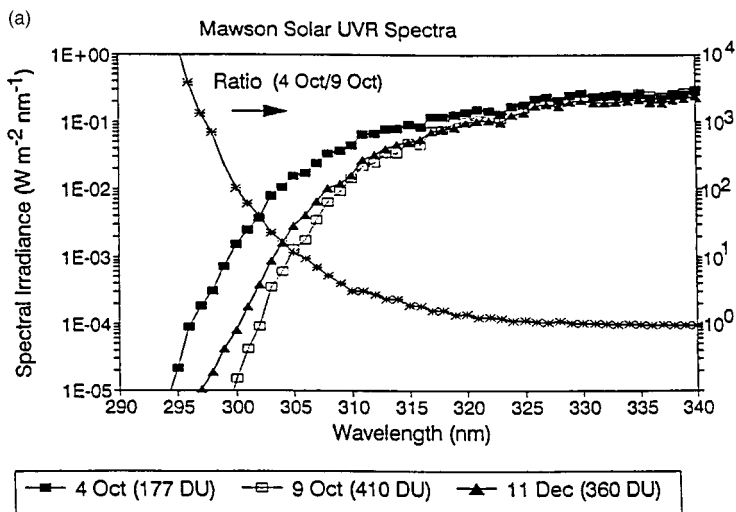
Figure 1.7. (a) The influence of the Antarctic ozone hole on the spectrum of solar radiation reaching the earth's surface at Mawson Station. Spectra are shown for the same solar angle but with varying amounts of column O_3. The loss of O_3 allows shorter, more energetic wavelengths to penetrate the atmosphere altering the ratios of UV-B to UV-A and to PAR. (b) The effect of the Antarctic ozone hole on the energy of UV-B radiation impacting marine environments. An approximate five-fold increase in UV-B is shown for a day under the ozone hole (Roy *et al.*, 1994).

Frederick, 1994). This phenomenon is known as the cloud edge effect and is due to scattering from the sides of cumulus clouds.

In a study in Antarctica, Gautier *et al.* (1994) reported a higher correlation of surface UV-B with cloud transmittance than with ozone levels. They also showed that cloud transmittance correlated with the ratio of DNA-effective UV (heavily weighted in UV-B) to UV-A during part of the study. This suggested that cloud might alter the radiation spectrum; however, the authors believed this effect would be small compared to alterations produced by ozone reductions.

Lubin & Jensen (1995) have attempted to compare the large variability in UV radiation resulting from cloud affects to trends in UV resulting from ozone reduction. This study was conducted on a global scale with satellite information and radiative transfer models. Their study suggested that large areas of the globe will experience upward trends in erythema and plant damage-effective UV that are significant relative to interannual variability due to cloud cover. The time frame for these trends to become significant over the background variability is 10 to 100 years, depending on location, from the onset of ozone reduction (*circa* 1980).

1.3.1.4 Season and latitude

Season and latitude play an important role in the attenuation of solar radiation by controlling solar zenith angles and thereby the thickness of the air column through which radiation must pass before reaching the ground (Madronich, 1993). For example, a change in solar zenith angle from 55° to 75° implies a doubling of air mass. Solar radiation, including UV-B, is consequently highest and least variable in the tropics and decreases at higher latitudes (Figure 1.8). The combination of higher solar angles and the global distribution of ozone (excluding depletion) enhances the attenuation and the truncation of shorter UV-B wavelengths such that latitudes above 55° never experience the intensity or integrated daily dose common between 0° and 30°. Indeed, even under severe ozone depletion, UV irradiance in Antarctic is less than that prevailing at the equator. However, high latitude ecological systems have developed under less intense UV regimes and may not be readily adaptable to large increases in intensity or shifts in the spectrum (Weiler & Penhale, 1994).

1.3.2   Attenuation in the water column

1.3.2.1 Surface reflection

The attenuation of solar radiation by the water column begins when light strikes the water surface. The penetration of light into the water column
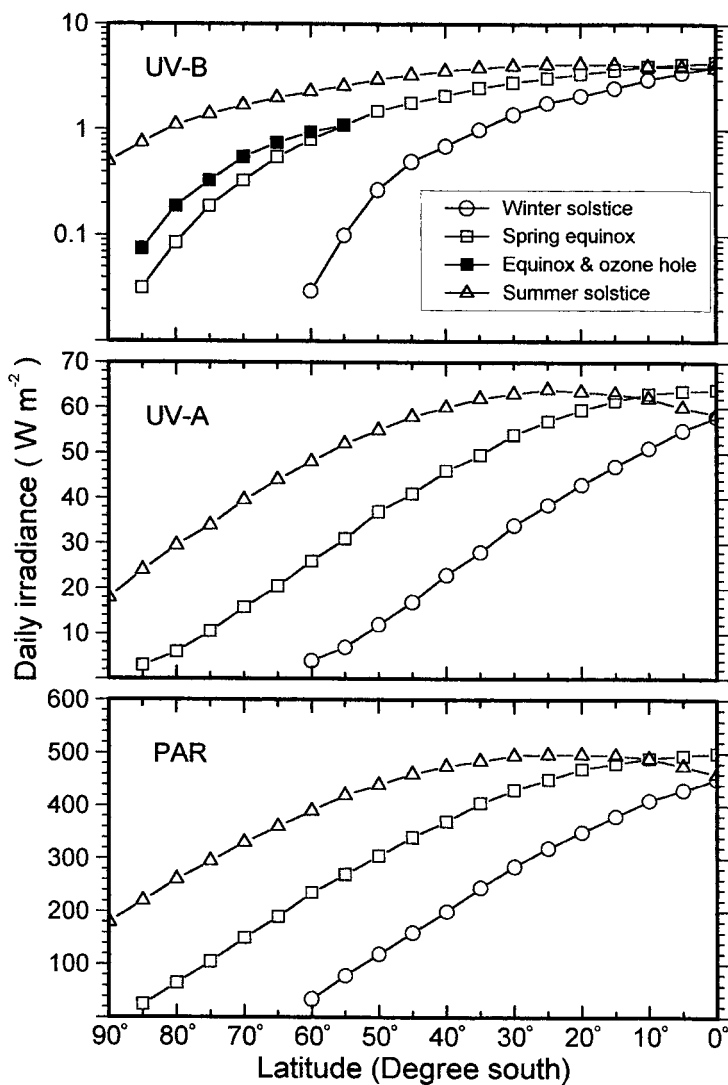
Figure 1.8. The influence of latitude and season on the solar energy at the earth's surface. Highest total energy and highest UV energy are at the equator, but the largest seasonal variability occurs at high latitudes. PAR, photosynthetically available radiation. (Adapted from Holm-Hansen *et al.*, 1993.)

can be diminished by reflection at the surface. For direct solar radiation and a smooth water surface, the percentage of light reflected can be calculated with the angle of the incident light (90° − solar elevation) and the relative refractive index of water. The computed reflectance as a percentage of incoming radiation for such conditions is given in Table 1.1. However, due to atmospheric effects, the solar radiation at the sea surface is composed of both direct and diffuse (i.e. sky) radiation. Theoretical calculations indicate that if all the radiation reaching the water surface were diffuse radiation, then approximately 6.6% would be reflected (Jerlov, 1976). Actual measurements (including a small contribution due to backscatter out of the water) show that diffuse radiation is reflected to an extent between 6% and 11% (Neumann & Pierson, 1966). Diffuse radiation is present to some extent in all solar radiation at ground level due to atmospheric scattering and its effect on reflection can be seen even under clear sky conditions (Table 1.1; Campbell & Aarup, 1989). On the other hand, there is still a direct component of solar radiation under heavily overcast skies and thus some variations in reflection due to changing solar elevations can be expected for all sky conditions (Neumann & Pierson, 1966).

Thus far, the assumption has been made that the sea surface is perfectly smooth, but observations demonstrate that this is seldom the case. Wind-roughened surfaces influence reflection because of changes in the angle of incidence for incoming light due to waves and changes in the nature of the air–sea interface through the production of bubbles and white-caps. Higher wind speeds tend to increase reflectance of direct solar radiation from high solar elevations, but the effect is minimal (Jerlov, 1976; Preisendorf & Mobley, 1986). At low solar elevations (< 20°), however, increasing wind speed significantly reduces direct reflectance by producing lower average incidence angles (Figure 1.9). The reflectance of

Table 1.1. Percentage reflectance of direct and global radiation from a smooth water surface as a function of solar elevations (h), angle of incidence = 90° − h

Solar elevation (h)	90°	60°	50°	40°	30°	20°	10°	5°
% Reflectance of direct radiation	2.0	2.1	2.4	3.4	5.9	13.3	34.9	58.3
% Reflectance of global radiation (direct + diffuse) clear sky	3	3	3	4	6	12	27	42

Data from Jerlov, 1976.

diffuse radiation is also reduced with increasing wind speed from 6.6% at $0 \, m \, s^{-1}$ to 4.7% at $20 \, m \, s^{-1}$ (Preisendorf & Mobley, 1986). White-caps and surface bubbles tend to increase all reflectance, but their lifetimes are relatively short and their influence is minor under most conditions (Kirk, 1994a).

   The influence of air–sea transmittance on the spectral quality of underwater light is even more equivocal and relatively little work has been done in this area. The percentage of total (global) radiation that is composed of sky (diffuse) radiation is influenced by solar elevation, atmospheric clarity and cloud cover. On average as a manifestation of the inverse relationship between scattering and wavelength, the violet end of the spectrum contains a higher percentage of sky radiation than the red end of the spectrum. A wavelength dependence for reflectance of solar radiation could therefore be expected, particularly at low solar elevations, due to differences in the reflectance of direct and diffuse light (Jerlov, 1976). UV at ground level exhibits a high ratio of diffuse to direct radiation regardless of sky conditions and thus reflection of these wavelengths is relatively invariant with changes in solar angles (Jerlov,
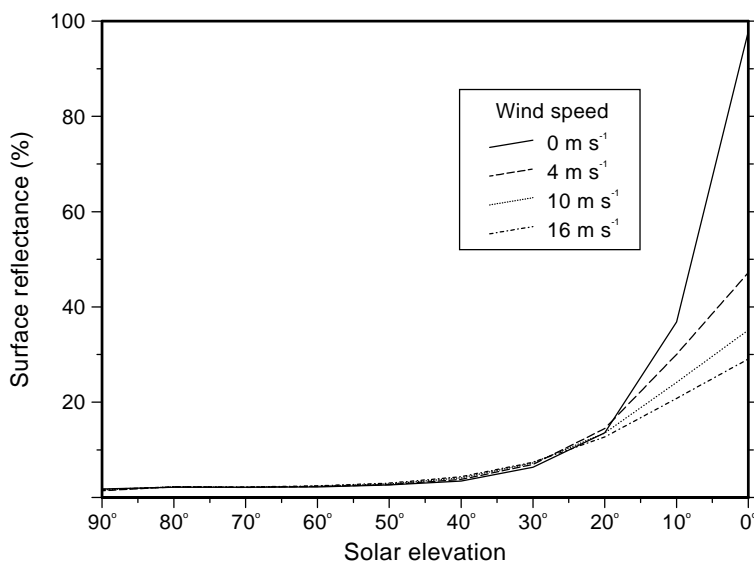

Figure 1.9.   Percentage reflectance of direct radiation as a function of solar elevation for various wind speeds. (Data from Austin, 1974.)

1976). Although this differential reflection of wavelengths could influence the spectral quality of underwater light, especially at high latitudes with lower average sun elevations, the extent of its influence is difficult to determine and is probably negligible in comparison with spectral variability in incident solar radiation (Campbell & Aarup, 1989).

1.3.2.2 Scattering and absorption

Once solar radiation has entered the water column, it is subject only to two physical processes: scattering and absorption. These two processes are dependent on the optical properties of the water column, which are functions of the scattering and absorption by water itself and that of particles and dissolved substances in the water. Optical properties can be divided into two classes as follows (Preisendorf, 1976):

1. Inherent properties are independent of the incident light field, but are spectrally dependent. They include index of refraction, coefficients for attenuation, absorption and scattering, and the volume scattering function.
2. Apparent properties such as irradiance attenuation depend on the inherent properties and the radiance distribution of the light field. Consequently irradiance attenuation depends on numerous factors and extrapolation among water bodies is not unambiguous.

For radiation in the solar spectrum, irradiance attenuation by water itself is little affected by the dissolved inorganic salts or gases in seawater. Therefore, the inherent optical properties of pure seawater itself will not vary with salinity but are slightly influenced by temperature and pressure. (Pure seawater refers to seawater containing all the common inorganic salts but lacking any suspended particles or dissolved organic constituents.) Both pure water and pure seawater have high absorptivity at the red and IR end of the spectrum. However, contrary to earlier published values, recent work has shown that the attenuation of UV wavelengths by water itself is very low, being about $0.01\,\mathrm{m}^{-1}$ (Kirk, 1994a). Therefore, the contribution of irradiance attenuation by pure seawater itself serves to shift the spectral distribution of underwater light towards the blue end of the spectrum relative to the solar spectrum (for more details, see Chapter 2).

The variation in irradiance attenuation for seawater experiencing a constant light field can thus be attributed to variations in scattering and absorption (i.e. inherent optical properties) due to dissolved organic constituents together with living and non-living particles (Figure 1.10). Reviews of aquatic radiative transfer are available (Preisendorf, 1976;

Mobley, 1994; Kirk, 1994a). As in the atmosphere, scattering can influence the rate at which photons are absorbed, but a scattered photon is still able to interact within the aquatic ecosystem unless it is backscattered out of the water column. Although, by definition, attenuation considers a scattered photon to be lost from the main beam, only absorption actually removes a photon from the system. From an irradiance measurement standpoint, the scalar irradiance (E_o) will always be higher than downwelling irradiance (E_d) due to the influence of scattering. The most relevant optical parameter for the evaluation of vertical penetration of radiation into the water column is the vertical attenuation coefficient (K_d). If the water column is optically homogeneous, downwelling irradiance can be related to K_d by:

$$E_{d\lambda}(z) = E_{d\lambda}(0)e^{-K_{d\lambda}z} \tag{1.3}$$

where $E_{d\lambda}(z)$ is downwelling irradiance at λ at depth z, $E_{d\lambda}(0)$ is downwelling irradiance at λ just below the surface and $K_{d\lambda}$ is vertical attenuation coefficient of λ at z in m^{-1}. The value of K_d is a result of all the
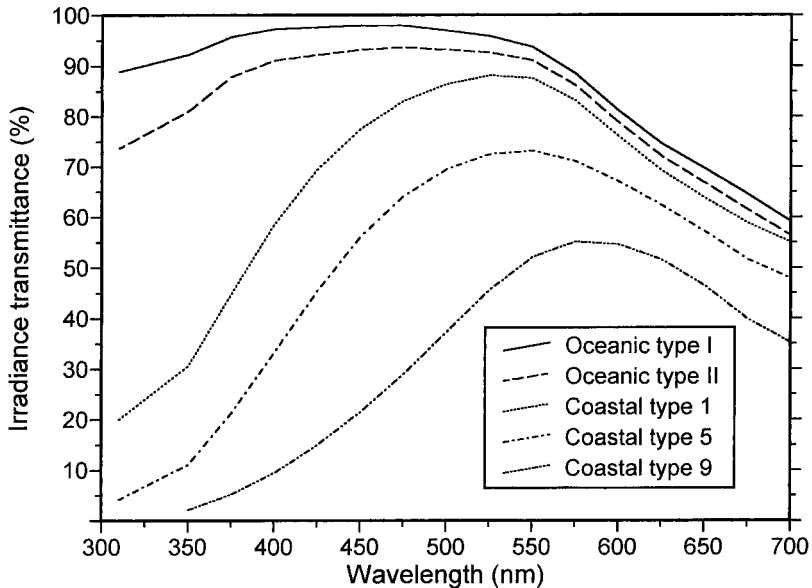

Figure 1.10. Percentage transmittance per metre for downward irradiance in various types of marine waters as classified by Jerlov (1976). Differences in transmittance can be attributed to variations in dissolved and suspended material in the various water types. (Data from Jerlov, 1976.)

radiative transfer processes in the water column and is determined mainly by the inherent optical properties (Kirk, 1994a). By using field analyses and computer modelling, Kirk (1994a) has defined an empirical relationship for the value of K_d in natural waters:

$$K_d = 1/\mu_o(a^2 + G(\mu_o)ab)^{1/2} \qquad (1.4)$$

where μ_o is the cosine of the refracted solar beam just below the surface, a is the absorption coefficient, b is the scattering coefficient and $G(\mu_o)$ is a coefficient whose value is determined by the shape of the scattering phase function, which specifies the angular distribution of scattering.

The UV absorbance coefficient for natural waters on has been shown to be highly dependent on the concentration of dissolved organic material (DOM), also known as humic material, yellow substance, gelbstoff, and chromophoric DOM (Smith & Baker, 1979; Kirk, 1994b). The characteristic absorbance spectra for DOM are very low at the red end of the spectrum and rise exponentially with decreasing wavelength in the UV. Particulate material with humic substances adsorbed onto the surface show the same general absorbance spectrum. Modelling of freshwater systems has shown that the UV absorbance coefficient for the water column can be fairly well determined by measuring DOM levels (measured as dissolved organic carbon (DOC)) (Williamson *et al.*, 1996). However, DOC concentrations and their relative contribution to absorption coefficients in seawater are usually much lower than in freshwater systems and a predictive model for seawater based solely on DOC concentrations is not feasible. Numerical models for radiative transfer (Mobley *et al.*, 1993) and empirical models based on DOC and chlorophyll levels (Smith & Baker, 1981; Baker & Smith, 1982) are effective at predicting average optical parameters, but require incident irradiance to determine the underwater light field. Examination of the empirical models and extrapolation from freshwater systems leads to the generalisation that coastal waters with higher concentrations of terrestrially derived DOC should have higher UV absorbance coefficients than open ocean water. It is also important to note that the UV absorbance coefficients for living particulate material can be equal to or greater than that of DOC and, therefore, phytoplankton themselves contribute to the attenuation of UV in the water column (self-shading). In contrast to the absorption coefficient, the scattering contribution to K_d can be reasonably estimated for both fresh and seawater from turbidity measurements (Kirk, 1985).

Once K_d has been measured or estimated for a particular water body, it